

CHITOSAN NANOPARTICLES MEDIATED DELIVERY OF MIR-106B-5P TO BREAST CANCER CELL LINES MCF-7 AND T47D

LEONNY DWI RIZKITA^{1,3}, YSRAFIL^{1,2}, RONNY MARTIEN⁴, INDWIANI ASTUTI^{1*}

¹Department of Pharmacology and Therapy, Faculty of Medicine, Public Health and Nursing, Universitas Gadjah Mada, Yogyakarta 55281, Indonesia, ²Department of Pharmacy, Health Polytechnic of Gorontalo, Ministry of Health, Gorontalo, Indonesia. ³Master in Biomedical Sciences Program, Faculty of Medicine, Public Health and Nursing, Universitas Gadjah Mada, Yogyakarta 55281, Indonesia, ⁴Department of Pharmaceutical Chemistry, Faculty of Pharmacy, Universitas Gadjah Mada, Yogyakarta 55281, Indonesia
Email: indwiani@gmail.com

Received: 16 Sep 2020, Revised and Accepted: 19 Oct 2020

ABSTRACT

Objective: The development of nanomedicine, such as miRNA transfection to cancer cells, has widely gained interest in the past decade. Unfortunately, miRNA tends to decay easily by the cellular enzymatic process and requires a carrier. As a cationic biopolymer, chitosan is widely known as a non-viral vector. However, research about chitosan as a miRNA delivery system remains limited. This study aimed to investigate the effect and characters of synthetic miRNA loaded chitosan nanoparticles on breast cancer cell lines.

Methods: To obtain the nanocomplex, chitosan-antimiR-106b-5p was formulated using natrium tripolyphosphate through ionic gelation methods. The nanochitosan formula was characterized by using gel electrophoresis; Nano Quant for encapsulation of entrapment quantification; morphology appearance as viewed by Scanning Electron Microscope (SEM), nanochitosan size analysis; *in vitro* analysis using MCF-7 and T47D breast cancer cell lines; *in silico* prediction of possible gene target; polymerase chain reaction analysis and gel electrophoresis for E2F1/GAPDH expression.

Results: The efficiency entrapment value was 96.7 %, particle size analysis was 458±11.79 nm, and polydispersity index (PDI) was 0.65±0.07, with spherical morphology as viewed in SEM. There was no significant difference between the nanochitosan supplemented group and the control group in MCF-7 cells ($p=0.067$). However, the ratio of E2F1 to GAPDH was significantly lower than the control group after nanochitosan anti-miR-106b-5p was loaded at concentration 140 nmol ($p=0.022$) and 35 nmol ($p=0.016$).

Conclusion: Our nanochitosan formula is non-toxic to use in MCF-7 cell lines. Most importantly, as the formula was conjugated to synthetic anti-miR-106b-5p, the E2F1 expression decreased.

Keywords: Chitosan, Nanoparticle, miR-106b-5p, Breast cancer, E2F1

© 2021 The Authors. Published by Innovare Academic Sciences Pvt Ltd. This is an open access article under the CC BY license (<http://creativecommons.org/licenses/by/4.0/>)
DOI: <http://dx.doi.org/10.22159/ijap.2021v13i1.39749>. Journal homepage: <https://innovareacademics.in/journals/index.php/ijap>

INTRODUCTION

miRNA therapy has gained popularity recently, with many studies focused on evaluating the dysregulated level of this short-chain non-coding RNA by correlating them with altered expression of various genes [1]. Cancer is on the top of the priority list due to having the highest morbidities and mortalities reported every year [2]. In 2040, the World Health Organization (WHO) estimates the global burden of cancer will rise by approximately fifty percent from 18.1 million in 2018 to 27.9 million in which 2.1 million cases are caused by female breast cancer [3–5]. In carcinogenesis, the abnormal level of intracellular miRNA could affect cellular growth and proliferation, differentiation, apoptotic, and cell cycle to tissue development [6–8]. Similar to other gene therapies, miRNA expression could be transfected by using the synthetic oligonucleotides either as a mimic or antagonist [9]. Unfortunately, most gene therapies encounter similar challenges, especially in how to envelope the genes safely accompanied by their release to targeted cells precisely [10].

To answer the challenge regarding the delivery system, scientists have also begun to develop various vectors to encapsulate these genes [11]. Nanomedicine in gene therapy applies to specific genes' transporting mechanism not only in terms of size but also the packaged biochemical properties [12, 13]. One of the main advantages derived from drug-based nanoparticles is its ability in enhancing the therapeutic level and achieving the desired pharmacological effect, especially in malignancy. Drug toxicity is also part of the widely discussed challenges. Achieving the precise dosage without affecting normal cells is partly correlated with the delivery system [14–16]. In cancer, nanoparticles that carry drugs to genes could also be designed to reach the cancer cells without affecting the normal cells since their size allows them to penetrate the cells more effectively [17–19]. To ensure its precise ability requires a safe, less immunogenic and biodegradable carrier. Although the viral vector is currently the most preferable, it still has inconvenient side

effects such as immunogenicity, oncogenicity and the limited DNA size that it can uptake [20, 21]. More strategies are being developed with better advantages, such as cationic polymers [22]. The popularity of cationic biopolymers is shown by better capacity to be modified and ability to package certain genes. Although polyethyleneimine (PEI) has strong gene complexation and high transfection efficiency, studies reported its level of toxicity is higher than chitosan [11, 14].

Chitosan is a biopolymer that is widely used for medicinal purposes [23]. Chitosan is obtained by alkaline deacetylation of chitin, which is derived from crustaceans of marine arthropods or insects. The natural characteristic of chitosan is its positively charged surface and is considered perfect as a carrier for gene therapy [21]. In an acidic environment, chitosan can form nanoparticles and is able to interact with negatively charged molecules such as miRNA [24]. Several studies have reported chitosan as an effective nanocarrier for gene therapy. siRNA in PEG-chitosan nanocarriers successfully penetrated the blood-brain barrier to reach glioblastoma cells effectively [19, 25]. Using the xenograft model, miR-34a encapsulated with chitosan was able to downregulate various metastatic genes, including MET, Axl, and c-Myc in prostate cancer cell lines [26]. In one study reported by Ysrafil in 2020 also evaluated the HIF1 α expression in the ovarian cancer cell line, SKOV3, after miR-155-5p chitosan encapsulated transfection [27].

However, chitosan preparation has various applicable methods. Ionic gelation is the most commonly used method since it is cheaper and only requires simple stirring. The powder base chitosan must be dissolved in an acidic solution and a crosslinker must be further added for the final formulation [10, 27]. By supplementing the chitosan solution with sodium tripolyphosphate, the chitosan is ready to be conjugated with anionic particles [28, 29]. The purposes of this study were to characterize and evaluate the safety of chitosan encapsulation for synthetic anti-miR in MCF-7 cell lines then to inspect the E2F1 mRNA expression post-transfection in a p53-mutated cell line, T47D.

MATERIALS AND METHODS

Human MCF-7 and T47D breast cancer cells were obtained from ATCC (Virginia, USA) and maintained in high glucose Dulbecco's modified Eagle's medium supplemented with 10% fetal bovine qualified serum (Massachusetts, USA), 1% Penicillin-Streptomycin (Massachusetts, USA), and 0.5% amphotericin (Massachusetts, USA). AntimiR-106b-5p was obtained from Integrated DNA Technologies (Iowa, USA). The miRCURY RNA Cell and Plant Kit, Universal cDNA synthesis kit II 8-64 rxns Exiqon was purchased from Woburn, USA. The Infinite® 200 PRO NanoQuant was purchased from Horiba Scientific (New Jersey, USA). Thermal Cycler (96 Well Capacity) PCR Select Cycler™ II was purchased from California, USA, and agarose gel electrophoresis system was purchased from Mupid-One® (Dueren, Germany). Nanoparticles Size Analyzer Sz-100 was obtained from Horiba Scientific (New Jersey, USA). Medium molecular weight chitosan was purchased from Sigma Aldrich (Missouri, USA).

Ch-NP-antimiR-106b-5p preparation

The chitosan-nanoparticle/antimiR was formulated by ionic gelation as previously demonstrated by Ysrafil *et al.* and Suardi *et al.* in 2020 [27, 30]. It is begun by dissolving the medium molecular weight chitosan powder into 1% acetic acid with 24 h magnetic stirring. The solution later was pH adjusted to gain acid environment (pH 5.5) by adding 1 mol of NaOH. Then, to obtain 0.2% chitosan solution, acetate buffer pH 5 was added. The nanocomplex formula was later made by ionic gelation method by mixing 0.2% chitosan with sodium tripolyphosphate (5:1), then incubating for 5 min at room temperature. Next, 200 µl of the ready-to-use solution was conjugated with 200 µl of antimiR-106b-5p and incubated for 20 min at room temperature.

Efficiency of entrapment

Efficiency of entrapment of the chitosan encapsulated antimiR-106b-5p was obtained by measuring the free concentration of antimiR-106b-5p inside the formula. The Ch-NP-106b-5p was centrifugated for 15 min at 13000 g speed. The supernatant obtained was measured by its absorbance using The Infinite® 200 PRO NanoQuant. Then, the absorbance efficiency was formulated as follows by comparing the percentage of encapsulated miRNA to total miRNA [27, 31].

$$\frac{\text{Total miRNA} - \text{unencapsulated miRNA}}{\text{total miRNA}} \times 100\%$$

Ch-NP-antimiR-106b-5p morphology measurement

Chitosan antimiR-106b-5p nanocomplex was prepared as 3 µmol concentrate by diluting it into nuclease-free water as mentioned and referred to from Suardi *et al.* in 2020 [30]. To measure the size, a Nanoparticle Size Analyzer Horiba Sz-100 was used and to evaluate the morphology, Scanning Electron Microscope (SEM) was used.

Cell viability assay

We observed and analyzed the cells' tolerability toward the chitosan solution by using cytotoxic tests on MTT assay method [32]. T47D

and MCF-7 cells were seeded into 96 well plates with approximately 6×10^3 cells in each well plate, then incubated for 24 h at 37 °C and 5% CO₂. The next day, the media was removed from each well and the cells were given 100 µl of nanochitosan solution or high glucose DMEM only as the control group. MTT assay was then conducted after 24 h of incubation by pipetting 100 µl of 0.5 mg/ml MTT reagent in each well. After incubating the solution for 4 h, then 100 µl stopper solution (SDS 10% and 0.01 µl/l HCl) was added to dissolve the formazan crystals. The solution was then incubated again for the next 18 h in room temperature with the absence of light. The absorbance of each well was measured at a 595 nm wavelength using Micro Plate Reader (Bio-Rad Model 680 XR).

Genes target expression analysis

T47D cells were seeded about 5×10^4 each well into a 6 well plate. Following 24 h of incubation, nanochitosan encapsulated antimiR-106b-5p was then added to each well with three different concentrations and incubated again for the next 24 h [27]. Total RNA was isolated using miRCURY RNA Cell and Plant Kit according to the manufacturer's protocol. Total RNA concentrations were measured by NanoQuant at 260 to 280 nm wavelengths. To gain the reverse transcribed RNA, 10 ng of total RNA was synthesized by using Universal cDNA synthesis kit II 8-64 rxns according to the manufacturer's protocol. Quantification of E2F1 mRNA used the following primers: (forward: ACTCCTCGCAGATCGTCATCATCT; reverse: GGACGTTGGTGATGTCATAGAT), and GAPDH as housekeeping gene (forward: GGCAAATTCACGGCACAGT; reverse: AGATGGTGATGGGCTTCCC). The polymerase chain reaction (PCR) products were later run through 2% agarose gel electrophoresis. The bands were quantified using ImageJ software.

Statistical analysis

All the analyzed data were measured in triplicate and outcome values were presented as mean±standard deviation (SD). We compared the cells viability between the chitosan nanoparticles (Ch-NP) with miRNA loaded as the experiment group with the high glucose DMEM as the control group using Independent T-tests. Gene target expressions were analyzed with Independent T-tests. All presented data were analyzed using SPSS 25 software (SPSS Inc., Chicago, USA) and graphics were performed by GraphPad Prism 8.0. Statistical significance was set at $p < 0.05$.

RESULTS AND DISCUSSION

Efficiency of entrapment

To evaluate the presenting synthetic oligonucleotides encapsulated by the nanochitosan formula, we labeled both the naked and Ch-NP-antimiR-106b-5p with fluorochrome and ran it through 2% agarose gel electrophoresis for 15 min. As viewed from the GelDoc, the well from the naked antimiR showed in the background as a greyish white area between the dark backgrounds while the encapsulated antimiR was likely to stay at the base of the well (fig. 1A).



Fig. 1: (A) Agarose gel electrophoresis of chitosan/antimiRNA (1) Naked antimiR (2); (B) Efficiency of entrapment of the Ch-NP-antimiR-106b-5p as measured by NanoQuant and spherical morphology of nanochitosan was visualized by Scanning Electron Microscope, Abbreviation: Ch-NP-antimiR-106b-5p: Chitosan Nanoparticle antimiRNA-106b-5p

We also quantified the efficiency of entrapment using NanoQuant to measure the percentage of total miRNA encapsulated by the nanochitosan. Using the formula, the value of the efficiency of entrapment was 96.7% (fig. 1B). The obtained value indicated the total miRNA concentrations encapsulated by the chitosan nanocomplex through ionic gelation with sodium tripolyphosphate. The spherical morphology of the nanochitosan also has a meaningful contribution as viewed from SEM analysis, making it easily distinguishable (fig. 1B).

Morphology analysis of Ch-NP-antimiR-106b-5p

We conducted particle size analysis of the encapsulated antimiR-106b-5p to evaluate the nanocomplex formation by the chitosan. We obtained the size of nanoparticles 458 ± 11.79 nm with Polydispersity Index (PDI) 0.65 ± 0.07 (table 1). With PDI less than 0.7, the nanoparticles would likely distribute uniformly and this would strengthen their ability to reach the intracellular [33].

Table 1: Nanochitosan distribution and size analysis (n=3)

	Particle size	Polydispersity Index (PDI)
Ch-NP-antimiR-106b-5p	458 ± 11.79 nm	0.65 ± 0.07

Abbreviation: Ch-NP-antimiR-106b-5p: Chitosan Nanoparticle antimiRNA-106b-5p. (n=3) and data were given in mean \pm SD.

Cell viability after nanochitosan transfection

We performed the simplest and most effective calorimetric assay (3-(4,5-dimethyl-2-thiazolyl)-2,5-diphenyl-2H-tetrazolium bromide (methyl thiazolyl tetrazolium; MTT)) to identify the mitochondrial activity of cytochrome b and c from surviving cells. The living cells were shown as purple rings (formazan crystals). This assay was performed on all groups (chitosan supplemented cells and high glucose DMEM only). The absorbance values obtained later were analyzed and compared to the control group. We conducted an Independent T-tests test since our data were normally distributed. As observed by the absorbance values, there was no significant difference neither in the nanochitosan nor in the control group ($p=0.067$).

In silico identification of miRNA target prediction

Furthermore, we also conducted the bioinformatic analysis to predict the binding location of E2F1 mRNA toward the miR-106b-5p. As predicted by the tools, miR-106b-5p could recognize EF21 at base number 1972-1987 from the chromosome locus with logistic probability of 0.74. The near 1 value of logistic probability marked the highest confidence of the binding location.

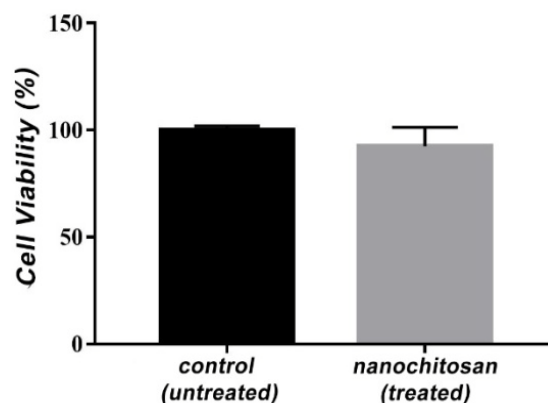


Fig. 2: MCF-7 cells, after given the chitosan nanoparticles, showed no significant cell diminishing (n=3). Data were presented as mean \pm SD with * $p < 0.05$ versus the control group (untreated cell line)

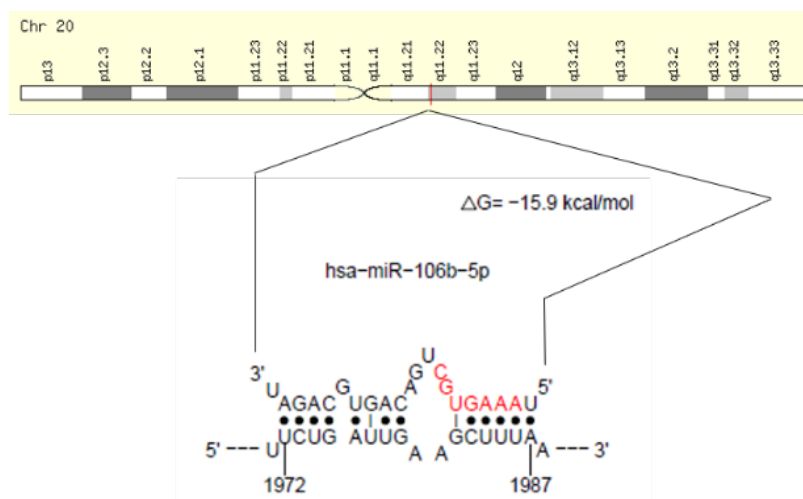


Fig. 3: In silico approach of miR-106b-5p-E2F1 recognition and binding prediction using STarMirDB combined with GeneCard

E2F1 mRNA expression analysis after Ch-NP-antimiR-106b-5p transfection to T47D cells

We measured the gene target expression by running the extracted RNA through PCR to predict the nanoparticles' ability to deliver the synthetic oligonucleotides intracellular into its functional location on T47D cells. The cells were seeded and incubated into 6 well plate for 24 h continued with antimiR-chitosan transfection for the next

24 h. The cDNA from each concentration group (140 nmol, 70 nmol, 35 nmol and control group) were diluted and mixed with the PCR MasterMix reagents (GoTaqGreen) then run through 2% gel agarose electrophoresis. As seen in fig. 4, E2F1/housekeeping gene GAPDH mRNA expression was significantly lower in all dosages given compared to the control group treated with free serum DMEM only (Independent T-test; $p < 0.05$) in two different concentrations: 140 nmol and 35 nmol.

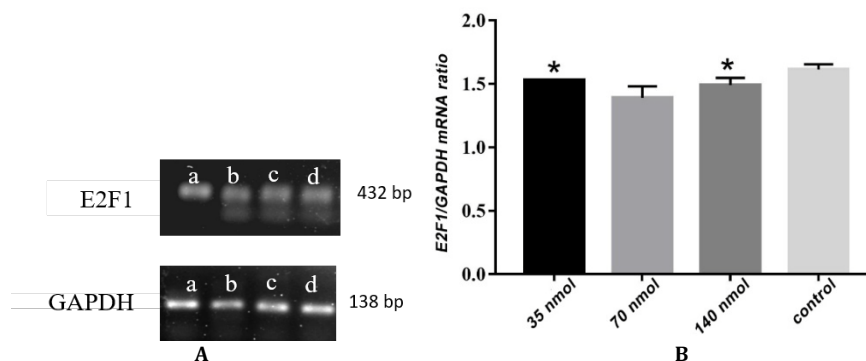


Fig. 4: (A) Electrophoresis band of endogenous E2F1/GAPDH mRNA level after Ch-NP-antimiR-106b-5p transfection given in three different concentrations: 35 nmol, 70 nmol and 140 nmol compared to control group. (B) endogenous E2F1/GAPDH mRNA level quantified by RT-PCR, from left to right at concentrations: (a) 35 nmol, (b) 70 nmol, (c) 140 nmol and (d) control group; (n=3). Data were presented as mean±standard deviation (SD) with *p<0.05 versus control group (untreated cell line)

Abbreviation: E2F1, E2F Transcription Factor 1; GAPDH, glyceraldehyde 3-phosphate dehydrogenase; RT-PCR, reverse transcription-polymerase chain reaction

Targeted therapy has become more desirable in the last few decades due to its great potential in solving numerous challenges that have occurred in efforts to eradicate certain diseases, especially cancer. The studies of miRNA have gained popularity since it belongs to non-coding RNA, which are able to interact with abundant target genes involved in tumorigenesis. It also could affect changes at the functional protein level [31]. Unfortunately, it is almost impossible to transfect the miRNA into the intracellular and penetrate the membranes safely. The dehydrogenase enzymes can decay it even before reaching the surface so it may lose efficiency due to its inability to conjugate with certain ligands. In terms of predicting the solution, many vectors have been developed to solve this problem and using biopolymers is another strategy to replace the highly immunogenic plasmid viral vector [14].

As an effective drug deliverer, the popularity of chitosan is well-known due to its ability to penetrate into the tight junction of cell membranes effectively, with low immunogenicity and biodegradability, while its polycationic character by nature makes it easy to interact with negative charged nucleic acids [15, 34]. To formulate the chitosan requires certain methods and ionic gelation simple complexation is the easiest technique. It is made by conjugating the chitosan with anionic multivalent triphosphate (TPP) as the crosslinker. The TPP will create strong binding flex with the amine molecules of chitosan to stabilize the matrix. In addition, TPP is less toxic compared to any other chemical crosslinker, such as glutaraldehyde [28, 35, 36]. In this study, we aimed to formulate the nanochitosan by using the medium molecular weight chitosan under an acidic environment. Molecular weight may affect the transfection ability and medium weight has notable advantages to induce better bioavailability since it carries more amines and hydroxyl molecules inside. The acidity of the dissolving solution also enhances the protonation among the amine molecules [36, 37].

A few studies suggested the optimal ratio of chitosan: TPP is about 6:1 (Morris *et al.*, 2011). Also, another study revealed the effective ratio for chitosan-PEG_{5k}: TPP: miRNA is 30:4:1 and optimized by fluorescence observation with DyS47 labelled miR-67 mimic. From this ratio, the obtained efficiency of encapsulation is 60 % [31]. However, as mentioned in one study by Al-Nemrawi *et al.* in 2018, the nanoparticles tend to form bigger sizes when the TPP was added up to 3 mg into the solution [38]. The change of ratio between the chitosan and TPP could also alter the particle size and PDI. It is expected to increase the particle growth after increasing the ratio from 25:5 to 25:10 as mentioned in a study by Hassan *et al.* in 2018 [39]. In this study, we used the nanochitosan formula optimized by Ysrafil *et al.* in 2020 with 5:1 ratio of chitosan: TPP. The optimization ratio was tested on SKOV3 cells using cellular uptake measurement by labelling the miRNA with FAM-conjugated label [27].

Furthermore, chitosan nanoparticle exact size could be affected by chitosan concentration. To obtain less than 500 nm nanoparticle

size, Katas *et al.* in 2013 reduced the concentration to about 0.05% [40]. Higher concentration (>0.25 %) may induce spontaneous coagulation of the formed particles as 1000 nm particles. To avoid the possibility of a bigger size, we used the optimized 0.2% chitosan concentration according to Ysrafil's study in 2020 [27]. However, the chitosan size particle also depends on the amount of TPP added in the ionic gelation methods [41]. We found the formula we referred from Ysrafil *et al.* in 2020 still showed the result was less than 500 nm nanoparticle size and was exactly 458 nm.

Nanochitosan transfection optimization has also been shown by anti-miR-fluorochrome labelling. The subtle illuminance on naked anti-miR implied some of the oligonucleotides retracted under the positive charge given from the electrophoresis. Meanwhile, the encapsulated anti-miR stayed at the well base, which indicated the predicted oligonucleotides entrapment by chitosan. The capsulation under polycationic chitosan engages the nucleic acids to form more positive charged particles. As the response, the electrostatic energy from the agarose gel failed to pull the nanocomplex downward. To analyze the predicted entrapment efficiency, we used the formula to measure the unencapsulated miRNA with NanoQuant. We obtained 96.7% of encapsulation efficiency from the nanocomplex formula. This high percentage may correlate with nearly completely condensate oligonucleotides by the nanochitosan matrix.

Results from the 24 h of incubation of MCF-7 cells after given 200 µl of the nanochitosan formula showed no significant cells diminishing compared to high glucose DMEM supplemented cells as the control group (fig. 2). This result implied that the cell viability remained normal and could grow. Compared to NaCl, unmodified chitosan has a lower toxicity value (LD₅₀: 16 g/kg, while LD₅₀ for NaCl is 3 g/kg) [14]. As reported by Kean and Thanou in 2010, median lethal dose (LD₅₀) and half-maximal inhibitory (IC₅₀) for chitosan and its derivatives in all cells model are approximately 0.2-2.5 mg/ml [42], which is much lower compared to any other biopolymer or liposome based vector.

We also assessed the effect of anti-miR chitosan encapsulation transfection on T47D cells after overnight incubation. Stender *et al.* in 2007 reported by using biochemical and bioinformatics analysis to MCF-7 and MDA-MB-231 cells, E2F1 gene is associated with E2 activity during tumor progression [43]. However, since p21 gene as the negative control is mostly suppressed by miR-106b-5p activity, the oncogene CIP2A could inhibit the phosphatase of phosphatase-tumor suppressor complex, PP21, and induces the E2F1 overexpression [44]. As shown in fig. 4, with the E2F1 relative expression toward the GAPDH as a stable housekeeping gene, the significant value was only marked on two different anti-miR concentrations, at the lowest and highest concentration, compared to the control group. Our *in silico* assessment showed the E2F1 is one of the strong gene targets of miR-106b-5p. E2F1 is a transcription factor for numerous genes involved for DNA

replications [45]. During the cell cycle, cyclin-dependent kinase (CDK) phosphorylated the tumor suppressor protein retinoblastoma protein (pRB) and released E2F1 for various genes, which could be expressed during DNA synthesis, including mitosis [46]. Some studies also suggested the transcription of miR-106b-25 involved E2F1 activity [47]. T47D cells as part of the luminal A type cell line along with MCF-7 expressed abundant ER α in the cytosolic membranes and the receptors as suggested by Louie *et al.* in 2010, while E2F1 as a cell cycle transcription gene could be modulated by the ER α together with Sp-1 protein [48]. These findings indicate the plausible reasons for why our E2F1 level only decreased slightly.

CONCLUSION

In summary, we concluded that chitosan nanoparticle could be used as an effective transfecting courier for nucleic acid such as microRNA into the cells without showing toxicity toward the cells. Furthermore, *in vitro* study revealed that anti-miR-106b-5p conjugated with chitosan nanoparticle could induce the expression of E2F1 mRNA after transfection.

To verify the strong correlation after treatment, endogenous miR-106b-5p expression should be measured and the values plotted with the mRNA target. Fluorescence-labelled synthetic oligonucleotides (FITC) is also another alternative to evaluate the miRNA-loaded nanochitosan uptake into cells.

ACKNOWLEDGEMENT

Thank you to Dr. med. dr. Indwiani Astuti as supervisor and Dr. rer. nat. Ronny Martien, M. Si as co-supervisor.

FUNDING

Partially supported by authors.

AUTHORS CONTRIBUTIONS

First author is a postgraduate student, second author a consultant, third author a co-supervisor and fourth author a supervisor.

CONFLICT OF INTERESTS

The authors declare that they have no conflict of interest.

REFERENCES

- Kaban K, Salva E, Akbuga J. *In vitro* dose studies on chitosan nanoplexes for microRNA delivery in breast cancer cells. *Nucleic Acid Ther* 2017;27:45–55.
- Sabit H, Cevik E, Tombuloglu H, Farag K, Said OAM, Shaimaa E, *et al.* miRNA profiling in MCF-7 breast cancer cells: seeking a new biomarker. *J Biomed Sci* 2019;8:1–9.
- Bray F, Ferlay J, Soerjomataram I, Siegel RL, Torre LA, Jemal A. Global cancer statistics 2018: GLOBOCAN estimates of incidence and mortality worldwide for 36 cancers in 185 countries. *CA Cancer J Clin* 2018;68:394–424.
- American Cancer Society. Global cancer facts and fig. 4th edition; 2018.
- World Health Organization. Breast cancer; 2018. Available from: <https://www.who.int/cancer/prevention/diagnosis-screening/breast-cancer/en/> [Last accessed on 26 Aug 2020]
- Mollaeh H, Safaralizadeh R, Rostami Z. MicroRNA replacement therapy in cancer. *J Cell Physiol* 2019;2:1–16.
- Nigussie Mekuria A, Degaga Abdi A, Mishore KM. MicroRNAs as a potential target for cancer therapy. *J Cancer Sci Ther* 2018;10:152–61.
- Ahmad J, Hasnain SE, Siddiqui MA, Ahamed M, Musarrat J. microRNA in carcinogenesis and cancer diagnostics: new paradigm biogenesis of miRNA. *Indian J Med Res* 2013;137:680–94.
- Peng B, Chen Y, Leong KW. microRNA delivery for regenerative medicine. *Adv Drug Delivery Rev* 2015;88:108–22.
- Karimi M, Avci P, Ahi M, Gazori T, Hamblin MR, Naderi Manesh H. Evaluation of chitosan-tripolyphosphate nanoparticles as a p-shRNA delivery vector: formulation, optimization and cellular uptake study. *J Nanopharmaceutical Drug Delivery* 2013;1:1–28.
- Arya G, Mankamna Kumari R, Sharma N, Gupta N, Chandra R, Nimesh S. Polymeric nanocarriers for site-specific gene

- therapy. In: Drug targeting and stimuli sensitive drug delivery systems; 2018. p. 689–714.
- Wicki A, Witzigmann D, Balasubramanian V, Huwyler J. Nanomedicine in cancer therapy: challenges, opportunities, and clinical applications. *J Controlled Release* 2015;200:138–57.
- Fluhmann B, Ntai I, Borchard G, Simoons S, Mühlebach S. Nanomedicines: the magic bullets reaching their target? *Eur J Pharm Sci* 2019;128:73–80.
- Cao Y, Tan YF, Wong YS, Liew MWJ, Venkatraman S. Recent advances in chitosan-based carriers for gene delivery. *Mar Drugs* 2019;17:1–21.
- Martien R, K Irianto ID, Farida V, Purwita Sari D. Perkembangan teknologi nanopartikel sebagai sistem penghantaran obat. *Maj Farm* 2012;8:133–44.
- Patra JK, Das G, Fraceto LF, Campos EVR, Rodriguez Torres MDP, Acosta-Torres LS, *et al.* Nano based drug delivery systems: recent developments and future prospects. *J Nanobiotechnol* 2018;16:1–33.
- Bahrami B, Hojjat Farsangi M, Mohammadi H, Anvari E, Ghalamfarsa G, Yousefi M, *et al.* Nanoparticles and targeted drug delivery in cancer therapy. *Immunol Lett* 2017;190:64–83.
- Xu X, Ho W, Zhang X, Bertrand N, Farokhzad O. Cancer nanomedicine: from targeted delivery to combination therapy. *Trends Mol Med*. 2015;21:223–32.
- Aftab S, Shah A, Nadhman A, Kurbanoglu S, Aysil Ozkan S, Dionysiou DD, *et al.* Nanomedicine: an effective tool in cancer therapy. *Int J Pharm* 2018;540:132–49.
- Ishii T, Okahata Y, Sato T. Mechanism of cell transfection with plasmid/chitosan complexes. *Biochim Biophys Acta Biomembranes* 2001;1514:51–64.
- Gascon R, del Pozo Rodriguez A, Solinis M. Non-viral delivery systems in gene therapy. In: Gene therapy-tools and potential applications; 2013. p. 3–34.
- Santos Carballal B, Aaldering LJ, Ritzeveld M, Pereira S, Sewald N. Physicochemical and biological characterization of chitosan-microRNA nanocomplexes for gene delivery to MCF-7 breast cancer cells. *Nat Publ Gr* 2015;5:13567.
- Naskar S, Koutsu K, Sharma S. Chitosan-based nanoparticles as drug delivery systems: a review on two decades of research. *J Drug Target* 2018;27:1–41.
- Mohammed MA, Syeda JTM, Wasan KM, Wasan EK. An overview of chitosan nanoparticles and its application in non-parenteral drug delivery. *Pharmaceutics* 2017;9:1–26.
- Ding Y, Shen SZ, Sun H, Sun K, Liu F, Qi Y, *et al.* Design and construction of polymerized-chitosan coated Fe₃O₄ magnetic nanoparticles and its application for hydrophobic drug delivery. *Mater Sci Eng C* 2015;48:487–98.
- Denizli M, Aslan B, Mangala LS, Jiang D, Rodriguez Aguayo C, Lopez Berestein G, *et al.* Chitosan nanoparticles for miRNA delivery. In: Bindewald E, Shapiro B, editors. RNA nanostructures: methods and protocols, methods in molecular Biology. 1st ed. Humana Press; 2017. p. 219–30.
- Ysrafil Y, Astuti I, Anwar LS, Martien R, Sumadi FAN, Wardhana T, *et al.* microRNA-155-5p diminishes *in vitro* ovarian cancer cell viability by targeting HIF1 α expression. *Adv Pharm Bull* 2020;10:630–7.
- Rahiemna A, Megafitrah M, Ramadhani P, Mustikawaty A, Martien R. Formulasi nanopartikel kitosan-PGV-0 dengan metode ionik gelasi. *J Saintifika Gadjah Mada* 2011;3:17–22.
- Adhyatmika A, Martien R, Ismail H. Preparasi nanopartikel senyawa pentagamavunon-0 menggunakan matriks polimer kitosan rantai sedang dan pengait silang natrium tripolifosfat melalui mekanisme gelasi ionik sebagai kandidat obat antiinflamasi. *Maj Farm* 2018;13:65.
- Suardi R, Ysrafil Y, Sesotiyosari S, Martien R, Wardana T, Astuti I, *et al.* The effects of combination of mimic miR-155-5p and antagonist miR-324-5p encapsulated chitosan in ovarian cancer SKOV3. *Asian Pacific J Cancer Prev* 2020;21:2603–8.
- Nguyen MA, Wyatt H, Susser L, Geoffrion M, Rasheed A, Duchez AC, *et al.* Delivery of microRNAs by chitosan nanoparticles to functionally alter macrophage cholesterol efflux *in vitro* and *in vivo*. *ACS Nano* 2019;13:6491–505.
- Riss T, Moravec R, Niles A, Duellman S, Benink H, Worzella T, *et al.* Cell viability assays. In: Markossian S, Sittampalam GS,

- Grossman A, Brimacombe K, Arkin M, Auld D, *et al.* editors. Assay guidance manual. Medical Bethesda (MD): Eli Lilly and Company and the National Center for Advancing Translational Sciences; 2004. p. 295–320.
33. Danaei M, Dehghankhold M, Ataei S, Hasanzadeh Davarani F, Javanmard R, Dokhani A, *et al.* Impact of particle size and polydispersity index on the clinical applications of lipidic nanocarrier systems. *Pharmaceutics* 2018;10:1–17.
 34. Ragelle H, Vanvarenberg K, Vandarmeulen G, Preat VP. Chitosan nanoparticles for siRNA delivery *in vitro*. In: Walker JM. editor. *Methods in molecular biology* (Clifton, NJ). Humana Press; 2016. p. 143–50.
 35. Katas H, Alpar HO. Development and characterization of chitosan nanoparticles for siRNA delivery. *J Controlled Release* 2006;115:216–25.
 36. Villegas Peralta Y, Lopez Cervantes J, Madera Santana TJ, Sanchez Duarte RG, Sánchez Machado DI, Martínez Macías M del R, *et al.* Impact of the molecular weight on the size of chitosan nanoparticles: characterization and its solid-state application. *Polym Bull* 2020. DOI:10.1007/s00289-020-03139-x
 37. Yang HC, Hon MH. The effect of the molecular weight of chitosan nanoparticles and its application on drug delivery. *Microchem J* 2009;92:87–91.
 38. Al-Nemrawi NK, Alsharif SSM, Dave RH. Preparation of chitosan-tpg nanoparticles: the influence of chitosan polymeric properties and formulation variables. *Int J Appl Pharm* 2018;10:60–5.
 39. Hassan NAFA, Sahudin S, Hussain Z, Hussain M. Self-assembled chitosan nanoparticles for percutaneous delivery of caffeine: preparation, characterization and *in vitro* release studies. *Int J Appl Pharm* 2018;10:172–85.
 40. Katas H, Raja MAG, Lam KL. Development of chitosan nanoparticles as a stable drug delivery system for protein/siRNA. *Int J Biomater* 2013;4:1–9.
 41. Morris GA, Castile J, Smith A, Adams GG, Harding SE. The effect of prolonged storage at different temperatures on the particle size distribution of tripolyphosphate (TPP)-chitosan nanoparticles. *Carbohydr Polym* 2011;84:1430–4.
 42. Kean T, Thanou M. Biodegradation, biodistribution and toxicity of chitosan. *Adv Drug Delivery Rev* 2010;62:3–11.
 43. Stender JD, Frasor J, Komm B, Chang KCN, Kraus WL, Katzenellenbogen BS. Estrogen-regulated gene networks in human breast cancer cells: involvement of E2F1 in the regulation of cell proliferation. *Mol Endocrinol* 2007;21:2112–23.
 44. Laine A, Westermarck J. Molecular pathways: harnessing E2F1 regulation for prosenescence therapy in p53-defective cancer cells. *Clin Cancer Res* 2014;20:3644–51.
 45. Petrocca F, Visone R, Onelli MR, Shah MH, Nicoloso MS, de Martino I, *et al.* E2F1-regulated microRNAs impair TGFβ-dependent cell-cycle arrest and apoptosis in gastric cancer. *Cancer Cell* 2008;13:272–86.
 46. Denechaud PD, Fajas L, Giralt A. E2F1, a novel regulator of metabolism. *Front Endocrinol (Lausanne)* 2017;8:1–8.
 47. Wei CY, Tan QX, Zhu X, Qin QH, Zhu FB, Mo QG, *et al.* Expression of CDKN1A/p21 and TGFBR2 in breast cancer and their prognostic significance. *Int J Clin Exp Pathol* 2015;8:14619–29.
 48. Louie MC, McClellan A, Siewit C, Kawabata L. Estrogen receptor regulates E2F1 expression to mediate tamoxifen resistance. *Mol Cancer Res* 2010;8:343–52.